

Transcription factor ETS1-mediated ECT2 expression promotes the malignant behavior of prostate cancer cells

BO ZHENG^{1*}, KUIFU CHEN^{1*}, XIN LIU², ZHENGHUA WAN¹, YULONG WU¹,
LIMING XU¹, JIGUANG XIAO¹ and JINQU CHEN¹

¹Department of Urology, The Fifth Hospital of Xiamen City, Xiamen, Fujian 361101, P.R. China;

²Department of Radiology, The Second Affiliated Hospital of Xiamen Medical College, Xiamen, Fujian 361000, P.R. China

Received January 24, 2024; Accepted May 22, 2024

DOI: 10.3892/ol.2024.14585

Abstract. Prostate cancer remains the most prevalent malignancy diagnosed in men worldwide. Epithelial cell transforming sequence 2 (ECT2) is an oncogene involved in the progression of human tumors. The present study aimed to explore the involvement of ECT2 in prostate cancer and its participation in the malignant progression of prostate cancer. ECT2 expression in prostate cancer cell lines was examined via reverse transcription-quantitative PCR and western blotting. The effects of knockdown of ECT2 expression in PC-3 cells on cellular biological behaviors, including proliferation, migration and invasion, were examined using Cell Counting Kit-8, colony formation, wound healing and Transwell assays. The glycolysis level was determined based on the lactate release, glucose uptake, oxygen consumption rate and extracellular acidification rate. The binding relationship between ECT2 and ETS1 was verified using luciferase reporter and chromatin immunoprecipitation assays. The results indicated that ECT2 was highly expressed in prostate cancer cell lines. Knockdown of ECT2 expression could inhibit cell proliferation, migration, invasion and glycolysis. In addition, the transcription factor ETS1 could directly bind to the ECT2 promoter and positively regulate ECT2 expression. These data were combined with the results of rescue experiments and demonstrated that the inhibitory effects of the knockdown of ECT2 expression on the malignant behavior and glycolysis of prostate cancer cells were partially reversed by ETS1 overexpression. In conclusion, ETS1 induced transcriptional upregulation of ECT2 and enhanced the malignant biological behaviors of prostate cancer cells, thereby promoting the progression of prostate

cancer. This evidence provides a theoretical basis for the treatment of prostate cancer.

Introduction

Prostate cancer remains the most prevalent malignancy diagnosed in men worldwide and the second most common cause of cancer-related death in men (1,2). In 2023, 288,300 new cases of prostate cancer and 34,700 prostate cancer-related deaths were expected in the United States (3). Due to the lack of apparent symptoms at the initial stages, patients with prostate cancer are generally diagnosed at an advanced stage with metastasis, which is associated with a high mortality rate (4). The androgen receptor is the main factor involved in the pathogenesis of prostate cancer. Therefore, androgen deprivation therapy (ADT) focusing on halting tumor growth has been the mainstay of prostate cancer treatment; however, the majority of patients develop castration resistance within 3 years following ADT failure, and even progress to the incurable metastatic castration-resistant prostate cancer stage, contributing to a poor 5-year survival rate (5-7). Therefore, it is urgently required to understand the detailed mechanisms underlying prostate cancer development, and to identify potential biomarkers of prostate cancer progression and novel therapeutic targets.

Epithelial cell transforming sequence 2 (ECT2), a guanine nucleotide exchange factor of Rho GTPases, is encoded by the human *ECT2* gene and is located on chromosome 3q26, a region prone to chromosome alterations in human tumors (8). Accumulating evidence has revealed that ECT2 serves a role in normal cellular activities, including cytokinesis and cell division, and participates in malignant transformation, tumor initiation and metastasis (9,10). ECT2 expression is upregulated in several types of human cancer, such as breast cancer, colorectal cancer, gastric cancer and esophageal squamous cell carcinoma, and the high ECT2 expression is associated with poor outcomes of patients with malignant tumors (11-14). ECT2 has been identified as an oncogene for human tumors. For instance, aberrant expression of ECT2 can drive colorectal cancer progression and growth (11), and ECT2 promotes the proliferation of glioma through stabilizing E2F transcription factor 1 (13). A previous study revealed that ECT2 expression is enhanced in human prostate cancer tissues, and this

Correspondence to: Mr. Jinqu Chen, Department of Urology, The Fifth Hospital of Xiamen City, 101 Min'an Road, Xiang'an, Xiamen, Fujian 361101, P.R. China
E-mail: chenjq202122@163.com

*Contributed equally

Key words: prostate cancer, epithelial cell transforming sequence 2, ETS1, aerobic glycolysis

expression is positively associated with tumor invasion and increased distant metastasis, suggesting that ECT2 is an independent prognostic marker of poor survival (15). Nevertheless, to the best of our knowledge, the involvement of ECT2 in the malignant progression of prostate cancer has not yet been addressed.

Therefore, the present study aimed to investigate the specific role of ECT2 in prostate cancer, and to explore the potential molecular mechanism, which will help identify novel targets and provide a theoretical basis for the treatment of prostate cancer.

Materials and methods

Bioinformatics analysis. The expression profile of ECT2 in prostate cancer was examined using the University of Alabama at Birmingham Cancer data analysis (UALCAN) portal (<http://ualcan.path.uab.edu>) (16) database based on 52 adjacent normal tissues and 497 tumor samples.

Cell culture. The RWPE-1 human normal prostate epithelial cell line was purchased from American Type Culture Collection and cultured in keratinocyte serum-free medium (Invitrogen; Thermo Fisher Scientific, Inc.) with 0.05 mg/ml bovine pituitary extract and 5 ng/ml human recombinant epidermal growth factor. The LNCaP, DU145, PC-3 and 22RV1 human prostate cancer cell lines were obtained from Procell Life Science & Technology Co., Ltd. LNCaP and 22RV1 cells were incubated with RPMI-1640 medium (Gibco; Thermo Fisher Scientific, Inc.) supplemented with 10% FBS (Gibco; Thermo Fisher Scientific, Inc.) and 1% penicillin/streptomycin mixture (HyClone; Cytiva). DU145 cells were incubated with Minimum Essential Medium (Procell Life Science & Technology Co., Ltd.) with 10% FBS and 1% penicillin/streptomycin, while PC-3 cells were incubated with Ham's F-12K medium (Procell Life Science & Technology Co., Ltd.) in the presence of 10% FBS and 1% penicillin/streptomycin. All cells were cultured at 37°C in a humidified incubator with 5% CO₂.

Western blotting. Total protein was isolated from PC-3 cells using RIPA lysis buffer (Beyotime Institute of Biotechnology). The protein concentration was determined using a BCA kit (Beyotime Institute of Biotechnology). The same amounts of proteins (30 µg/lane) were separated by electrophoresis using a 12% SDS-PAGE gel, and then transferred to polyvinylidene fluoride membranes. Following blocking with 5% nonfat milk at room temperature for 2 h, the membranes were probed with primary antibodies against ECT2 (1:1,000; cat. no. ab86604; Abcam), MMP2 (1:1,000; cat. no. 10373-2-AP; Proteintech Group, Inc.), MMP9 (1:2,000, cat. no. 30592-1-AP; Proteintech Group, Inc.), E-cadherin (1:10,000; cat. no. ab40772; Abcam), N-cadherin (1:10,000; cat. no. ab76011; Abcam), Vimentin (1:1,000; cat. no. ab92547; Abcam), hexokinase 2 (HK2; 1:1,000; cat. no. ab209847; Abcam), pyruvate kinase M2 (PKM2; 1:1,000; cat. no. ab85555; Abcam), lactate dehydrogenase A (LDHA; 1:1,000; cat. no. ab5248; Abcam), ETS1 (1:1,000; cat. no. ab186844; Abcam) and GAPDH (1:2,500; cat. no. ab9485; Abcam) at 4°C overnight. The membranes were incubated with HRP-conjugated goat anti-rabbit secondary antibody (1:5,000; cat. no. ab6721; Abcam) for 2 h

at room temperature. The blots were further developed using an enhanced chemiluminescence kit (Amersham; Cytiva) and semi-quantified using ImageJ software Version 1.52 (National Institutes of Health).

Reverse transcription-quantitative PCR (RT-qPCR). Total RNA was isolated from PC-3 cells using TRIzol® reagent (Invitrogen; Thermo Fisher Scientific, Inc.). The RNA concentration and purity were determined using a spectrophotometer (NanoDrop Technologies; Thermo Fisher Scientific, Inc.). Subsequently, 1 µg RNA was reverse-transcribed into cDNA using a First Strand cDNA Synthesis Kit (Sangon Biotech Co., Ltd.). The following conditions were used for RT: 42°C for 2 min, 37°C for 15 min and 85°C for 5 sec. Thereafter, SYBR Green qPCR Master Mix (Applied Biosystems; Thermo Fisher Scientific, Inc.) was used for the qPCR assay according to the manufacturer's instructions. The qPCR thermocycling conditions were as follows: Initial denaturation at 95°C for 10 min, followed by 40 cycles of 95°C for 15 sec, 55°C for 5 sec and 72°C for 10 sec. The primer sequences used in the present study were as follows: ECT2 forward, 5'-ACTACTGGGAGG ACTAGCTTG-3' and reverse, 5'-CACTCTTGTTCAT CTGAGGCA-3'; ETS1 forward, 5'-CCCGTACGTCCCCA CTCCT-3' and reverse, 5'-TGGGACATCTGCACATCCA-3'; and GAPDH forward, 5'-CAGGAGGCATTGCTGATGAT-3' and reverse, 5'-GAAGGCTGGGGCTCATTT-3'. The mRNA levels of the genes were calculated using the 2^{-ΔΔC_q} method (17). GAPDH was used as the internal control.

Cell transfection. Short hairpin RNAs (shs) (pGPU6 vector) targeting ECT2 (sh-ECT2-1 sense, 5'-CCGGGCTGAGCA TTCCCTTTCCATACTCGAGTATGGAAAGGGAATGCT CAGCTTTTTG-3' and antisense, 5'-AATTCAAAAAGC TGAGCATTCCCTTTCCATACTCGAGTATGGAAAGGG AATGCTCAGC-3'; and sh-ECT2-2 sense, 5'-CCGGCGGAA TGAACAGGATTTCTATCTCGAGATAGAAATCCTGTT CATTCCGTTTTTG-3' and antisense, 5'-AATTCAAAA ACGGAATGAACAGGATTTCTATCTCGAGATAGAAAT CCTGTTTCATTCCG-3') and ETS1 (sh-ETS1-1 sense, 5'-CCG GGTGCAGATGTCCCACTATTA ACTCGAGTTAATAGT GGGACATCTGCACTTTTTG-3' and antisense, 5'-AATTCA AAAAGTGCAGATGTCCCACTATTA ACTCGAGTTAAT AGTGGGACATCTGCAC-3'; and sh-ETS1-2: sense, 5'-CCG GTGTGAAACCATATCAAGTTAACTCGAGTTAACTTG ATATGGTTTTACATTTTTG-3' and antisense, 5'-AATTCA AAAATGTGAAACCATATCAAGTTAACTCGAGTTAAC TTGATATGGTTTTACA-3') were constructed by Shanghai GenePharma Co., Ltd., with scrambled shRNA (pGPU6) as the negative control (sh-NC; sense, 5'-CCGGCAACAAGA TGAAGAGCACCAACTCGAGTTGGTGCTCTTCATCTT GTTGTTTTTG-3' and antisense, 5'-AATTCAAAAACAACA AGATGAAGAGCACCAACTCGAGTTGGTGCTCTTCAT CTTGTTG-3'). The *Homo sapiens* ETS1 full-length open reading frame was amplified and inserted into a pcDNA3.1 vector to construct an ETS1 overexpression vector (oe-ETS1; Shanghai GenePharma Co., Ltd.). Empty pcDNA3.1 vector served as the negative control (oe-NC; Shanghai GenePharma Co., Ltd.). shs plasmids (50 nM) and/or oe-ETS1/oe-NC (15 nM) were transfected into PC-3 cells using Lipofectamine® 3000 reagent (Invitrogen; Thermo Fisher Scientific, Inc.) for

an incubation at 37°C for 6 h according to the manufacturer's instructions. PC-3 cells were not transfected served as the control. Following 48 h of culture at 37°C, the cells were harvested for subsequent experiments.

Cell proliferation assay. Cell proliferation was assessed using Cell Counting Kit-8 (CCK-8) and colony formation assays. For the CCK-8 assay, PC-3 cells were seeded into 96-well plates (1.0×10^4 cells/well) and incubated in a 5% CO₂ incubator at 37°C for the indicated durations (24, 48 and 72 h). CCK-8 solution (10 μl; Dojindo Molecular Technologies, Inc.) was added to each well for an additional incubation at 37°C for 2 h. The absorbance at 450 nm was recorded using a microplate reader. The relative cell viability (%) was calculated using the following formula: (absorbance in treated group-absorbance blank)/(absorbance in control group at 24 h-absorbance blank) x100.

In addition, PC-3 cells were seeded in 6-well plates (500 cells/well) and incubated in a 5% CO₂ incubator at 37°C for 2 weeks. The colonies (>50 cells) were fixed with methanol for 15 min at room temperature and stained with 0.1% crystal violet for 10 min at room temperature. Images were captured using light microscopy and colonies were observed by eye.

Assessment of cell migration and invasion. Cell migration was assessed using a wound healing assay. In brief, PC-3 cells were seeded in 6-well plates and incubated in a 5% CO₂ incubator at 37°C. When the cells reached 100% confluency, a single scratch wound was created using a 200-μl pipette tip. The plates were washed with PBS and subsequently cultured with serum-free medium for 24 h. Images were captured at 0 and 24 h using light microscopy. The cell migration rate (%) was calculated using the following formula: (0 h wound width -24 h wound width)/0 h wound width x100.

Cell invasion was detected using an 8-μm pore Transwell chamber (Corning, Inc.) precoated with Matrigel (BD Biosciences) for 30 min at 37°C. A total of 2.0×10^5 PC-3 cells were resuspended in serum-free medium and subsequently seeded into the upper Transwell chamber. The complete medium containing 10% FBS was plated in the lower chamber. Following incubation in a 5% CO₂ incubator at 37°C for 48 h, the non-invasive cells in the upper chamber were removed using a cotton swab. The invasive cells were fixed with methanol for 15 min at room temperature and stained with crystal violet for 10 min at room temperature. Finally, the images were observed using light microscopy and the invasive cells were counted using ImageJ software Version 1.52 (National Institutes of Health).

Measurement of lactate release, glucose uptake, oxygen consumption rate (OCR) and extracellular acidification rate (ECAR). The cell culture medium was harvested and the lactate release and glucose uptake were evaluated using lactate assay (cat. no. MAK064) and glucose uptake assay kits (cat. no. MAK542) (Sigma-Aldrich; Merck KGaA), respectively, according to the manufacturer's guidelines.

In addition, cells (1.0×10^4 cells/well) were seeded into XF96 cell culture microplates and incubated at 37°C overnight. The OCR and ECAR were detected using a Cell Mito Stress Test (cat. no. 103015-100) and Glycolysis Stress Test

Kit (cat. no. 103020-100), respectively, on a Seahorse XF96 Analyzer (all Agilent Technologies, Inc.), according to the manufacturer's guidelines.

Luciferase reporter assay. The promoter region of ECT2 (-2,000 to transcription start site) or mutant promoter region of ECT2 without ETS1-binding sites was cloned into the pGL3-Basic vector (Promega Corporation) to construct the luciferase reporter vectors. PC-3 cells were co-transfected with the luciferase reporter vectors and oe-NC/oe-ETS1 using Lipofectamine 3000 reagent. Following cell culture for 48 h post-transfection, the luciferase activity was detected using the Dual-Luciferase Reporter Assay System (Promega Corporation) according to the manufacturer's instructions, and normalized to *Renilla* luciferase activity.

Chromatin immunoprecipitation (ChIP) assay. The HumanTFDB (<http://bioinfo.life.hust.edu.cn/HumanTFDB#!/>) website was adopted to predict presumptive binding sites between the transcription factor ETS1 and the ECT2 promoter region, which was then verified using a ChIP assay, carried out using the SimpleChIP Enzymatic Chromatin IP Kit (Cell Signaling Technology, Inc.) according to the manufacturer's guidelines. In brief, PC-3 cells were fixed with 1% paraformaldehyde at 37°C for 10 min for crosslinking, quenched with 125 mM glycine at room temperature for 5 min, resuspended in SDS Lysis Buffer (MilliporeSigma) and subsequently sonicated into DNA fragments. After centrifugation at 12,000 x g for 5 min at 4°C, 100 μl of supernatant was incubated with 5 μg anti-ETS1 (cat. no. 14069; Cell Signaling Technology, Inc.) or anti-IgG (cat. no. 2729; Cell Signaling Technology, Inc.) antibodies. Protein A/G agarose beads (40 μl) (Santa Cruz Biotechnology, Inc.) were added to each IP reaction (100 μl) and incubated for 60 min at 4°C. The chromatin fragments were immunoprecipitated. After being washed with low-salt wash buffer, high-salt wash buffer and LiCl wash buffer, and being rinsed with TE buffer, the precipitated DNA was amplified and detected by qPCR as aforementioned.

Statistical analysis. Continuous variables are presented as the mean ± standard deviation from three repeats. Statistical analysis was conducted using an unpaired Student's t-test for two groups and one-way ANOVA with Tukey's post hoc test for more than two groups. The analysis was performed using GraphPad Prism software (version 8.0; Dotmatics). P<0.05 was considered to indicate a statistically significant difference.

Results

ECT2 expression is upregulated in prostate cancer. Using the UALCAN database, it was determined that the expression levels of ECT2 were significantly upregulated in prostate cancer tumor samples compared with normal samples (Fig. 1A). Subsequently, the expression levels of ECT2 were examined in normal prostate epithelial cells and prostate cancer cells to confirm the abnormal ECT2 expression in prostate cancer. As shown in Fig. 1B and C, the mRNA and the protein expression levels of ECT2 in prostate cancer cell lines (LNCaP, DU145, PC-3 and 22RV1 cells) were considerably higher than those in RWPE-1 cells. Among these cell lines, ECT2 expression

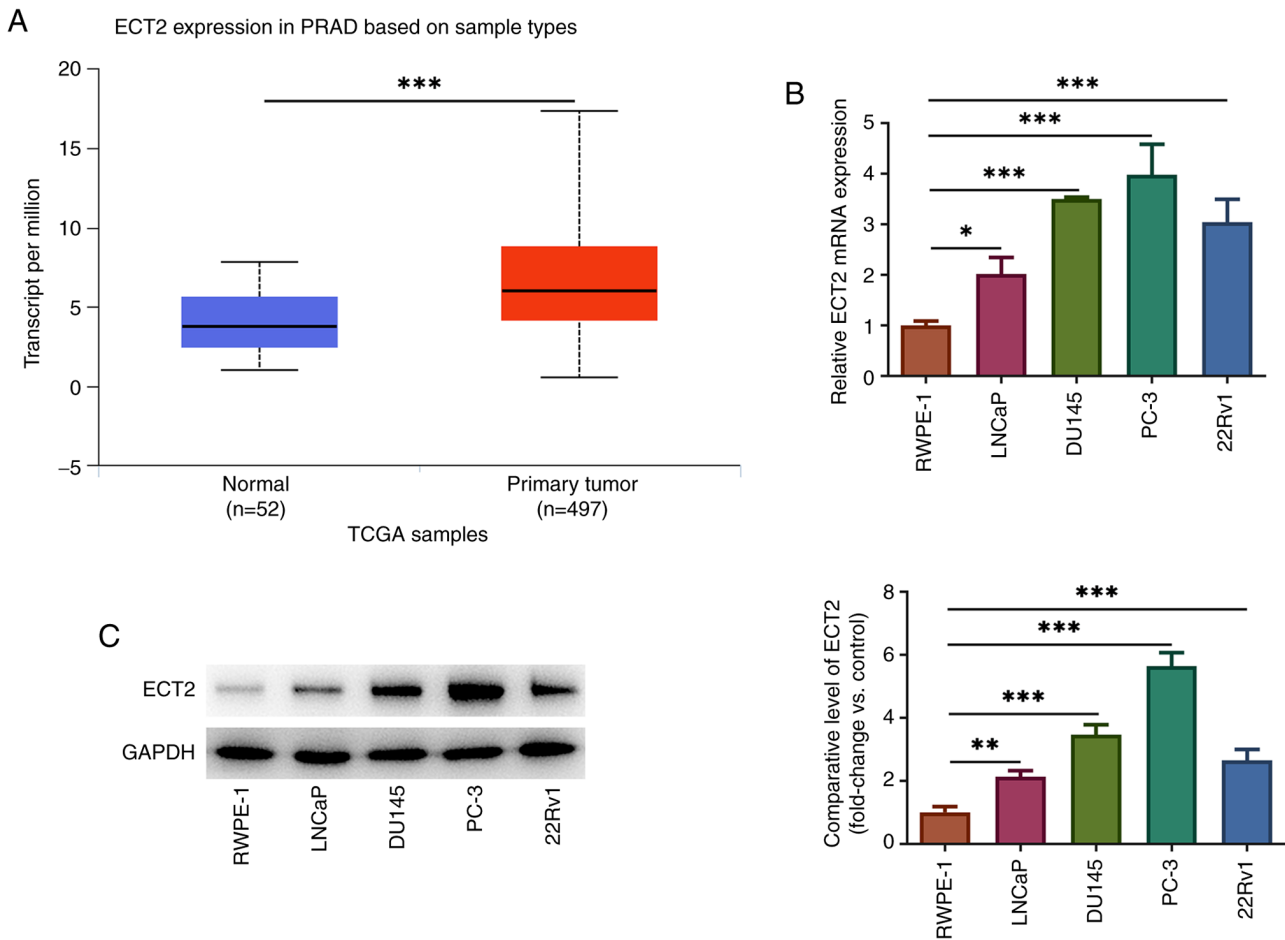


Figure 1. ECT2 expression is upregulated in prostate cancer. (A) ECT2 expression in prostate cancer from University of Alabama at Birmingham Cancer (UALCAN) website (<http://ualcan.path.uab.edu>). (B) mRNA levels of ECT2 in normal prostate epithelial and prostate cancer cells were examined using reverse transcription-quantitative PCR. (C) Protein expression levels of ECT2 in normal prostate epithelial and prostate cancer cells were examined using western blot analysis. * $P < 0.05$, ** $P < 0.01$ and *** $P < 0.001$. ECT2, epithelial cell transforming sequence 2; PRAD, prostate adenocarcinoma; TCGA, The Cancer Genome Atlas.

was highest in PC-3 cells. Therefore, PC-3 cells were used for subsequent experiments.

Knockdown of ECT2 expression reduces the proliferation, migration and invasion of PC-3 cells. To explore the regulatory role of ECT2 in prostate cancer, loss-of-function experiments were performed. As shown in Fig. 2A and B, the expression levels of ECT2 were significantly downregulated following transfection with sh-ECT2-1/2. The sh-ECT2-1 vector (designated sh-ECT2 hereafter) was used in subsequent experiments due to its superior transfection efficacy. The subsequent cellular behavior assays revealed that knockdown of ECT2 expression could effectively inhibit the proliferation of prostate cancer cells, as shown by the reduced colony formation and cell viability in the sh-ECT2 group compared with the sh-NC group (Fig. 2C and D). Furthermore, wound healing and Transwell assays revealed that knockdown of ECT2 expression could reduce the wound closure and number of invasive cells, indicating decreased migration and invasion of PC-3 cells following ECT2 knockdown (Fig. 2E and F). Additionally, the inhibitory effect of knockdown of ECT2 expression on the expression levels of MMP2 and MMP9 (invasion-related proteins) in PC-3 cells further confirmed the

anti-invasive effect of knockdown of ECT2 expression. In addition, the findings in Fig. 2G also revealed that knockdown of ECT2 expression significantly increased the expression levels of E-cadherin, a hallmark of epithelial cells, while significantly reducing the protein expression levels of N-cadherin and Vimentin (hallmarks of mesenchymal cells), suggesting that ECT2 knockdown in prostate cancer cells might retard the epithelial-mesenchymal transition which commonly occurs during cancer metastasis (18).

Knockdown of ECT2 expression restricts aerobic glycolysis of PC-3 cells. Prostate cancer cells can alter their glucose metabolism mode to aerobic glycolysis to meet the energy requirements for cell proliferation, migration, invasion and metastasis (19). Given that knockdown of ECT2 expression significantly inhibited the proliferation and invasion of PC-3 cells, additional experiments were performed to assess whether this effect was associated with changes in aerobic glycolysis. As shown in Fig. 3A and B, lactate release and glucose uptake were significantly decreased in the sh-ECT2 group compared with the sh-NC group. Accordingly, the decreased ECAR and increased OCR following sh-ECT2 transfection revealed that knockdown of ECT2 expression enhanced the glycolytic

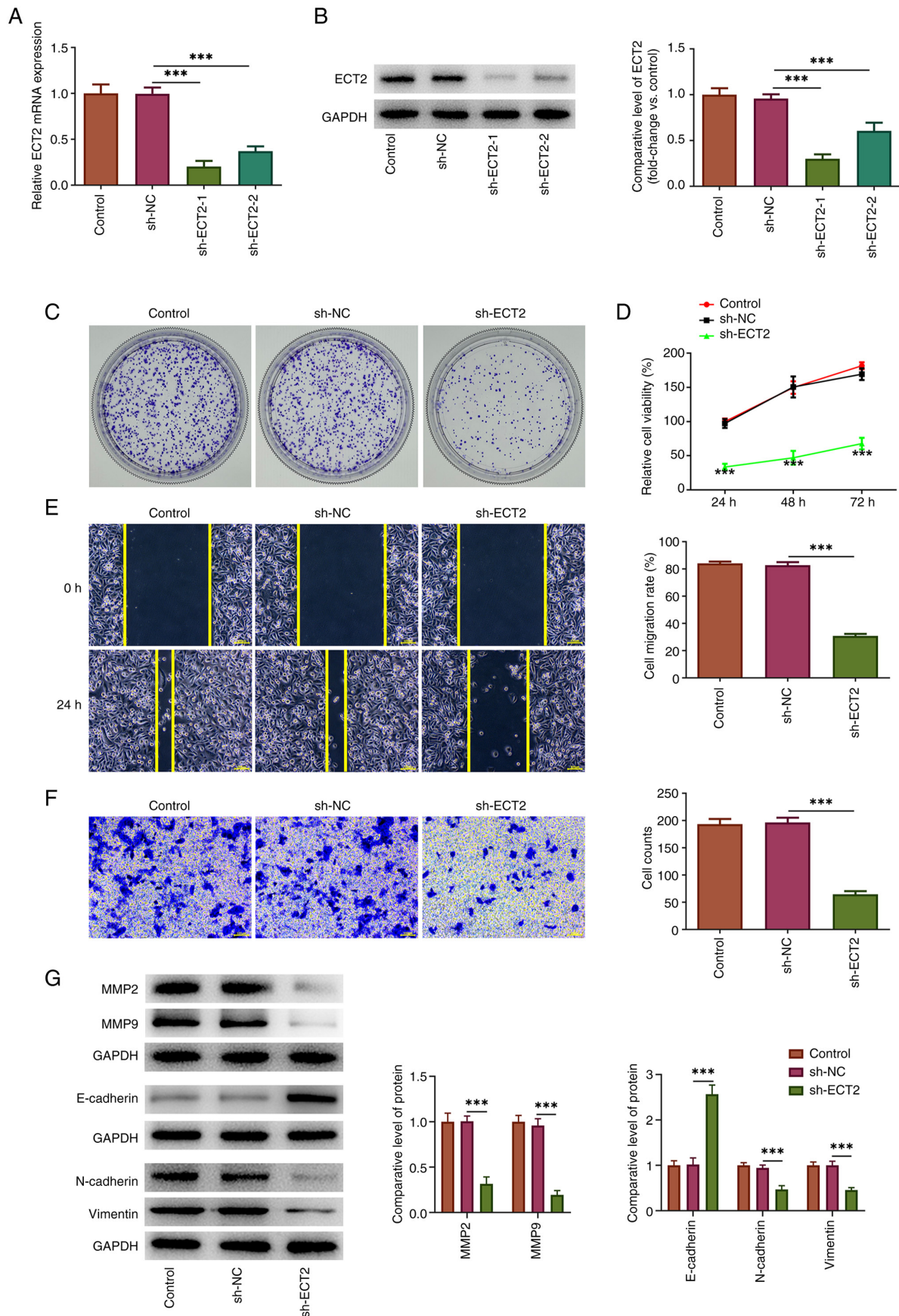


Figure 2. Knockdown of ECT2 expression inhibits the proliferation, migration and invasion of PC-3 cells. (A) PC-3 cells were transfected with sh-ECT2-1/2 or sh-NC, and the mRNA levels of ECT2 were examined using reverse transcription-quantitative PCR. (B) Protein expression levels of ECT2 were examined by western blot analysis. (C) A colony formation assay was conducted to examine cell proliferation. (D) Cell viability was assessed using a Cell Counting Kit-8 assay. ***P<0.001 vs. sh-NC. (E) A wound-healing assay was performed to assess cell migration. Scale bar, 100 μ m. (F) A Transwell assay was conducted to evaluate cell invasion. Scale bar, 100 μ m. (G) Relative protein expression levels were examined by western blot analysis. ***P<0.001. ECT2, epithelial cell transforming sequence 2; NC, negative control; sh, short hairpin RNA.

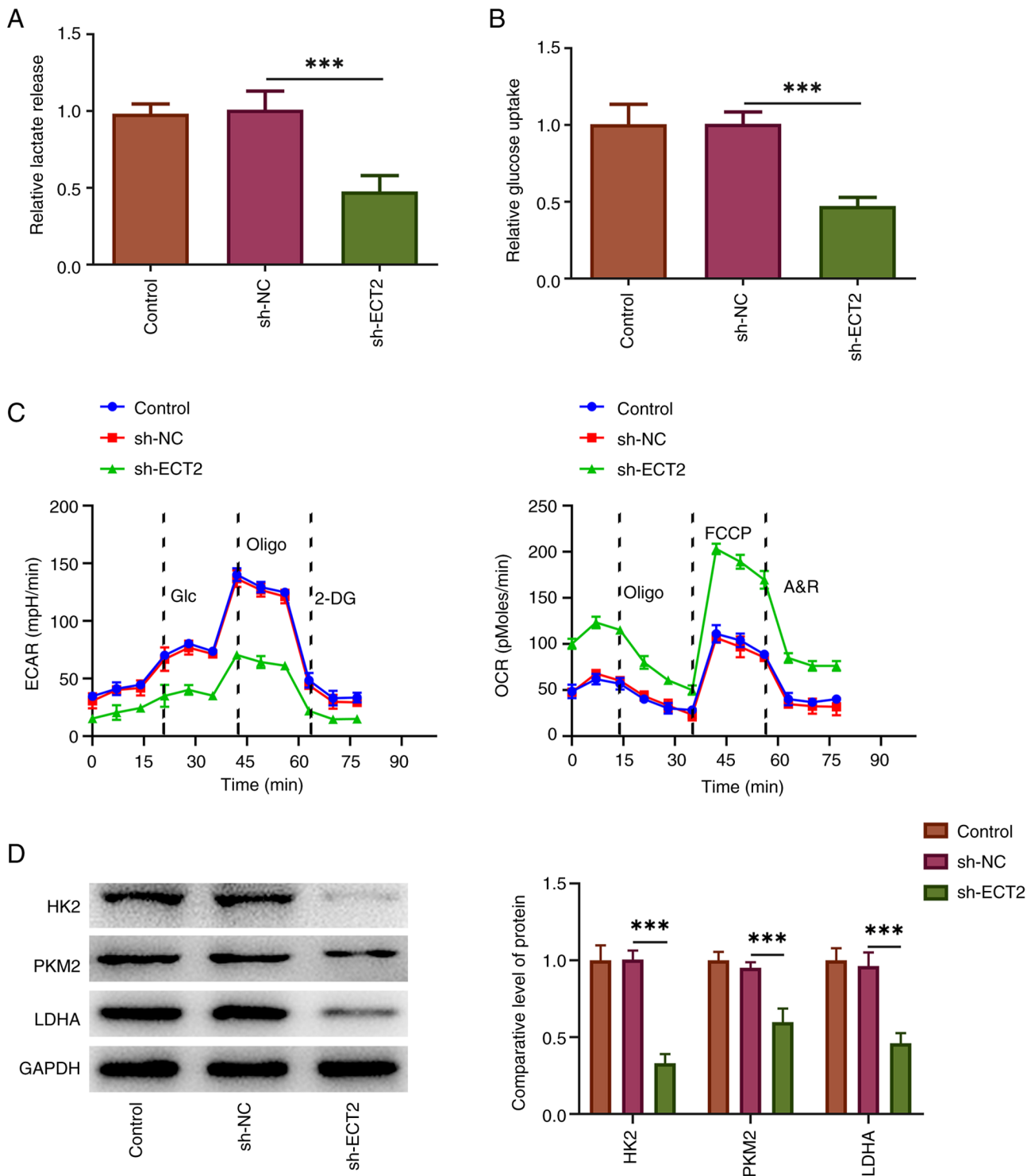


Figure 3. Knockdown of ECT2 expression restricts aerobic glycolysis in PC-3 cells. The cell culture medium was harvested and the (A) lactate release and (B) glucose uptake were examined using commercial kits. (C) The ECAR and OCR of PC-3 cells were assessed using a Seahorse XFe96 Analyzer to evaluate the glycolytic capacity and maximal respiration. (D) Western blotting was performed to examine the expression levels of several critical enzymes in the aerobic glycolysis process. *** $P < 0.001$. 2-DG, 2-deoxy-D-glucose; A&R, antimycin A/rotenone; ECAR, extracellular acidification rate; ECT2, epithelial cell transforming sequence 2; FCCP, carbonylcyanide-4-(trifluoromethoxy) phenylhydrazone; Glc, glucose; HK2, hexokinase 2; LDHA, lactate dehydrogenase A; NC, negative control; OCR, oxygen consumption rate; Oligo, oligomycin; PKM2, pyruvate kinase M2; sh, short hairpin RNA.

capacity, while it decreased ATP production and maximal respiration, suggesting that it impeded aerobic glycolysis in PC-3 cells (Fig. 3C). This was further verified by western blot analysis, which indicated that the expression levels of several critical enzymes in the aerobic glycolysis process, including LDHA, HK2 and PKM2, were significantly downregulated

following knockdown of ECT2 expression in PC-3 cells (Fig. 3D).

Transcription factor ETS1 binds to the ECT2 promoter and positively regulates ECT2 expression. Additional experiments were conducted to clarify the molecular mechanism of ECT2

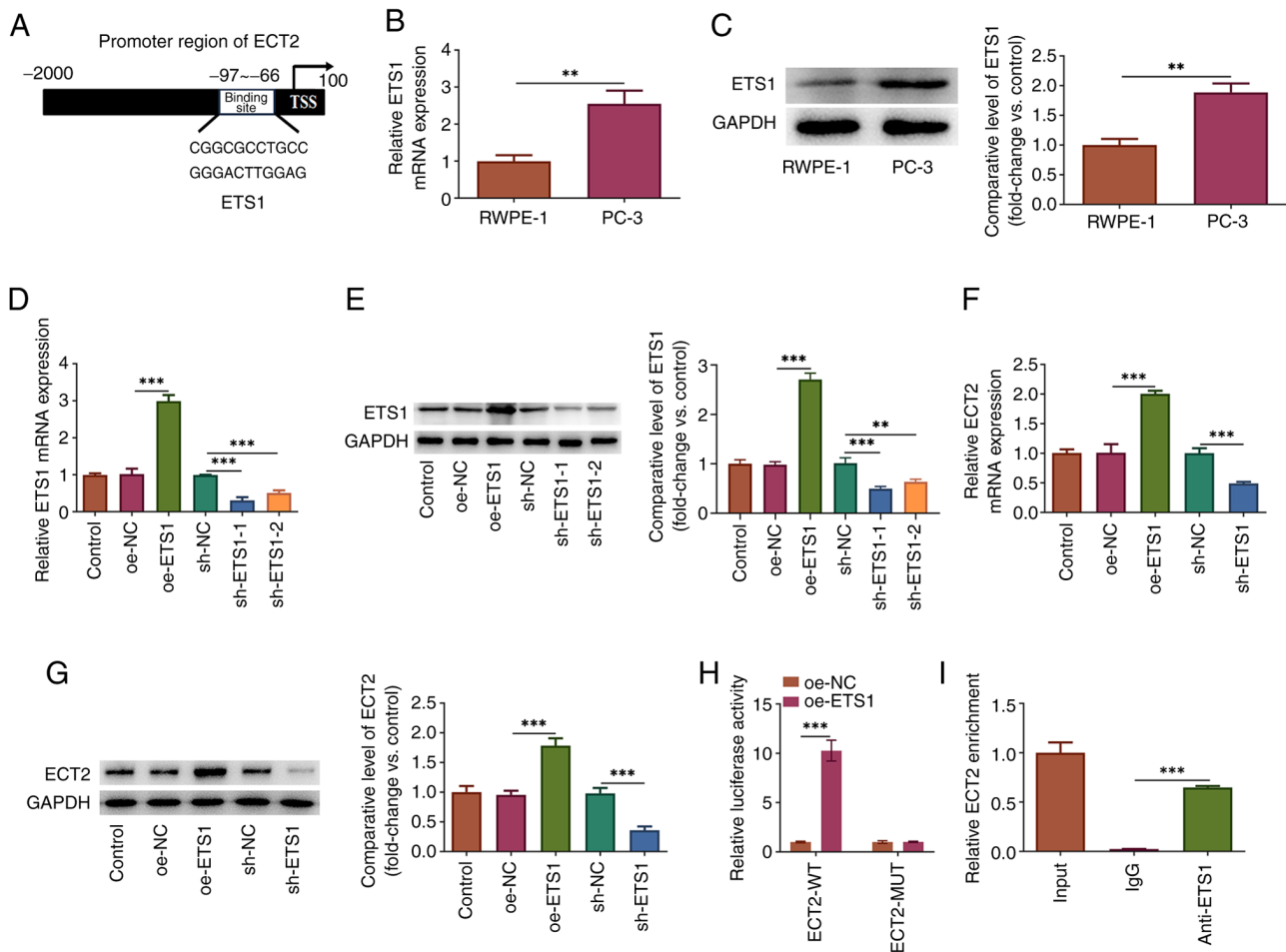


Figure 4. ETS1 transcriptionally binds to the ECT2 promoter and positively regulates ECT2 expression. (A) Predicted binding site between the transcriptional factor ETS1 and the ECT2 promoter. Expression levels of ETS1 in PC-3 and RWPE-1 cells were examined by (B) RT-qPCR and (C) western blot analyses. (D and E) PC-3 cells were transfected with oe-ETS1 to overexpress ETS1 or with sh-ETS1-1/2 to interfere with ETS1 expression. The mRNA and protein expression levels of ETS1 were examined using (D) RT-qPCR and (E) western blot analyses, respectively. The mRNA and protein expression levels of ECT2 were examined using (F) RT-qPCR and (G) western blot analyses, respectively. (H) The binding relationship between ETS1 and the ECT2 promoter was verified using a luciferase reporter assay. (I) A chromatin immunoprecipitation assay was conducted and the precipitated chromatin fragments were examined by qPCR. **P<0.01 and ***P<0.001. ECT2, epithelial cell transforming sequence 2; MUT, mutant; NC, negative control; oe, overexpression vector; RT-qPCR, reverse transcription-quantitative PCR; sh, short hairpin RNA; TSS, transcription start site; WT, wild-type.

and its regulation in prostate cancer cells. The HumanTFDB (<http://bioinfo.life.hust.edu.cn/HumanTFDB#!/>) website predicted that presumptive binding sites may exist between the transcription factor ETS1 and the ECT2 promoter region (Fig. 4A). It was observed that the expression levels of ETS1 were significantly upregulated in PC-3 cells compared with RWPE-1 cells (Fig. 4B and C). To explore the interaction between ETS1 and ECT2, PC-3 cells were transfected with oe-ETS1 plasmid to overexpress ETS1 or sh-ETS1-1/2 to interfere with ETS1 expression. sh-ETS1-1 was used for subsequent experiments due to its superior transfection efficacy (Fig. 4D and E). ETS1 overexpression significantly upregulated ECT2 expression, while knockdown of ETS1 expression significantly downregulated ECT2 expression (Fig. 4F and G), demonstrating that ETS1 could positively regulate ECT2. In addition, to confirm the binding site of ETS1 in the ECT2 promoter, luciferase reporter and ChIP assays were conducted. The data revealed that the luciferase activity in cells co-transfected with ECT2-wide-type (ECT2-WT) and oe-ETS1 was markedly increased in comparison to that

in cells co-transfected with ECT2-WT and oe-NC. There was no difference of the luciferase activity in cells with ECT2-mutant-type (Fig. 4H). Furthermore, the enrichment of precipitated chromatin fragments containing binding sites to the ECT2 promoter in the anti-ETS1 group was significantly higher than that in the IgG group (Fig. 4I). Therefore, these data confirmed that ETS1 could directly bind to the ECT2 promoter and positively regulate ECT2 expression at the transcriptional level in PC-3 cells.

Impact of knockdown of ECT2 expression on the malignant behavior and aerobic glycolysis of PC-3 cells is weakened by ETS1 overexpression. To verify the involvement of ETS1 underlying ECT2-mediated prostate cancer progression, gain- and loss-of-function experiments were conducted in PC-3 cells. As shown in Fig. 5A, PC-3 cells were transfected with sh-ECT2/sh-NC alone or co-transfected with sh-ECT2 and oe-ETS1/oe-NC, and the CCK-8 assay revealed that knockdown of ECT2 expression inhibited cell viability, which was partly reversed by additional ETS1

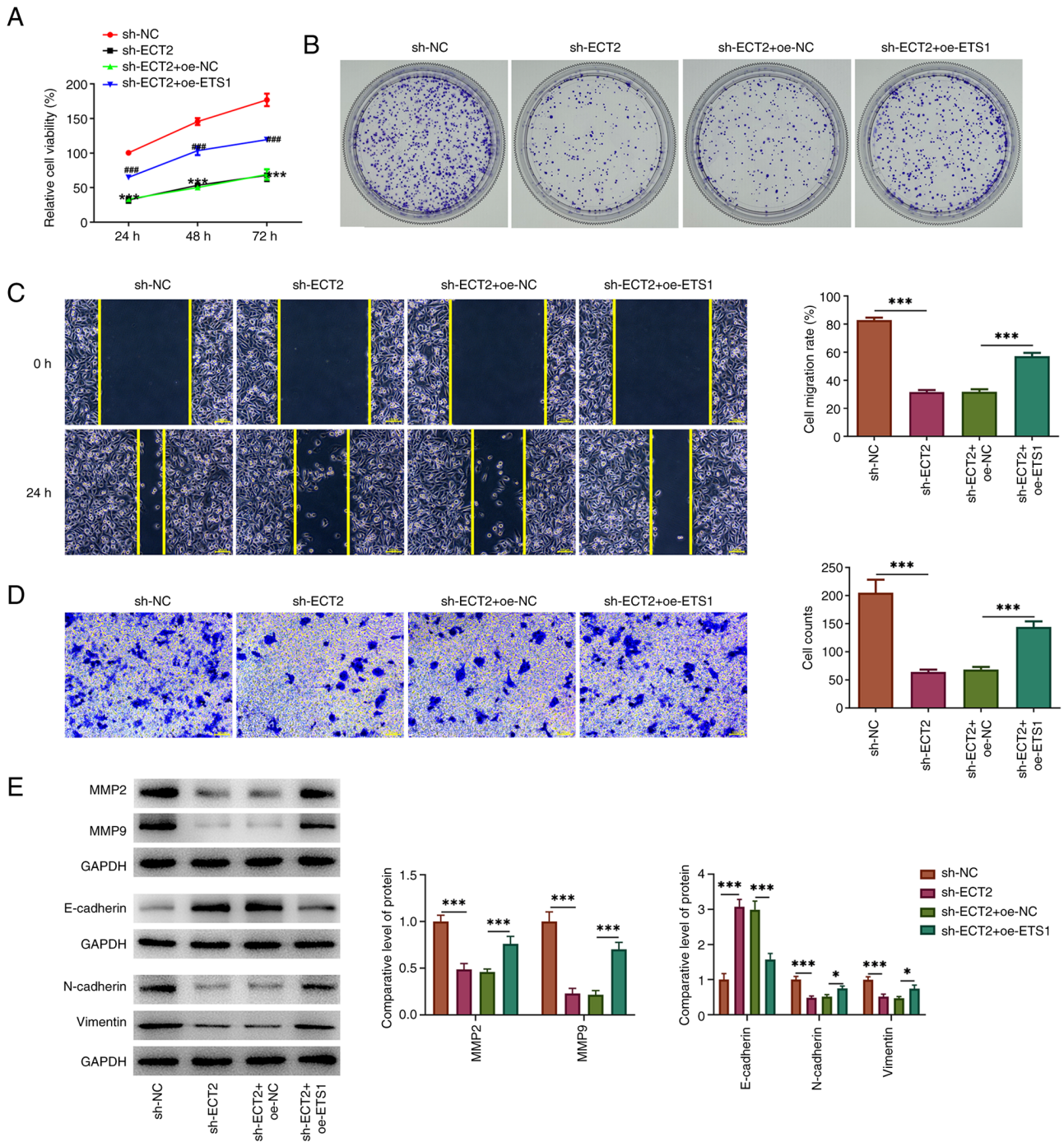


Figure 5. Impact of knockdown of ECT2 expression on proliferation, migration and invasion of PC-3 cells is weakened by ETS1 overexpression. (A) PC-3 cells were transfected with sh-ECT2/sh-NC alone or co-transfected with sh-ECT2 and oe-ETS1/oe-NC, and a Cell Counting Kit-8 assay was performed to examine cell viability. *** $P < 0.001$ sh-ECT2 vs. sh-NC; ### $P < 0.001$ sh-ECT2 + oe-ETS1 vs. sh-ECT2 + oe-NC. (B) A colony formation assay was conducted to examine cell proliferation. (C) A wound healing assay was performed to assess cell migration. Scale bar, 100 μm . (D) A Transwell assay was performed to evaluate cell migration. Scale bar, 100 μm . (E) Relative protein expression was examined by western blot analysis. * $P < 0.05$ and *** $P < 0.001$. ECT2, epithelial cell transforming sequence 2; NC, negative control; oe, overexpression vector; sh, short hairpin RNA.

overexpression. Knockdown of ECT2 expression-caused reduction in colonies was partly abolished following ETS1 overexpression (Fig. 5B). Subsequently, wound healing and Transwell assays revealed that the inhibitory effects of knockdown of ECT2 expression on cell migration and invasion were partly reversed by ETS1 overexpression (Fig. 5C and D). Furthermore, simultaneous transfection with sh-ECT2 and oe-ETS1 significantly increased the

protein expression levels of MMP2, MMP9, N-cadherin and Vimentin and decreased the protein expression levels of E-cadherin compared with those following transfection with sh-ECT2 and oe-NC (Fig. 5E). In addition, simultaneous transfection of the cells with sh-ECT2 and oe-ETS1 significantly increased lactate release and glucose uptake compared with transfection with sh-ECT2 and oe-NC. This was accompanied by upregulated ECAR and downregulated

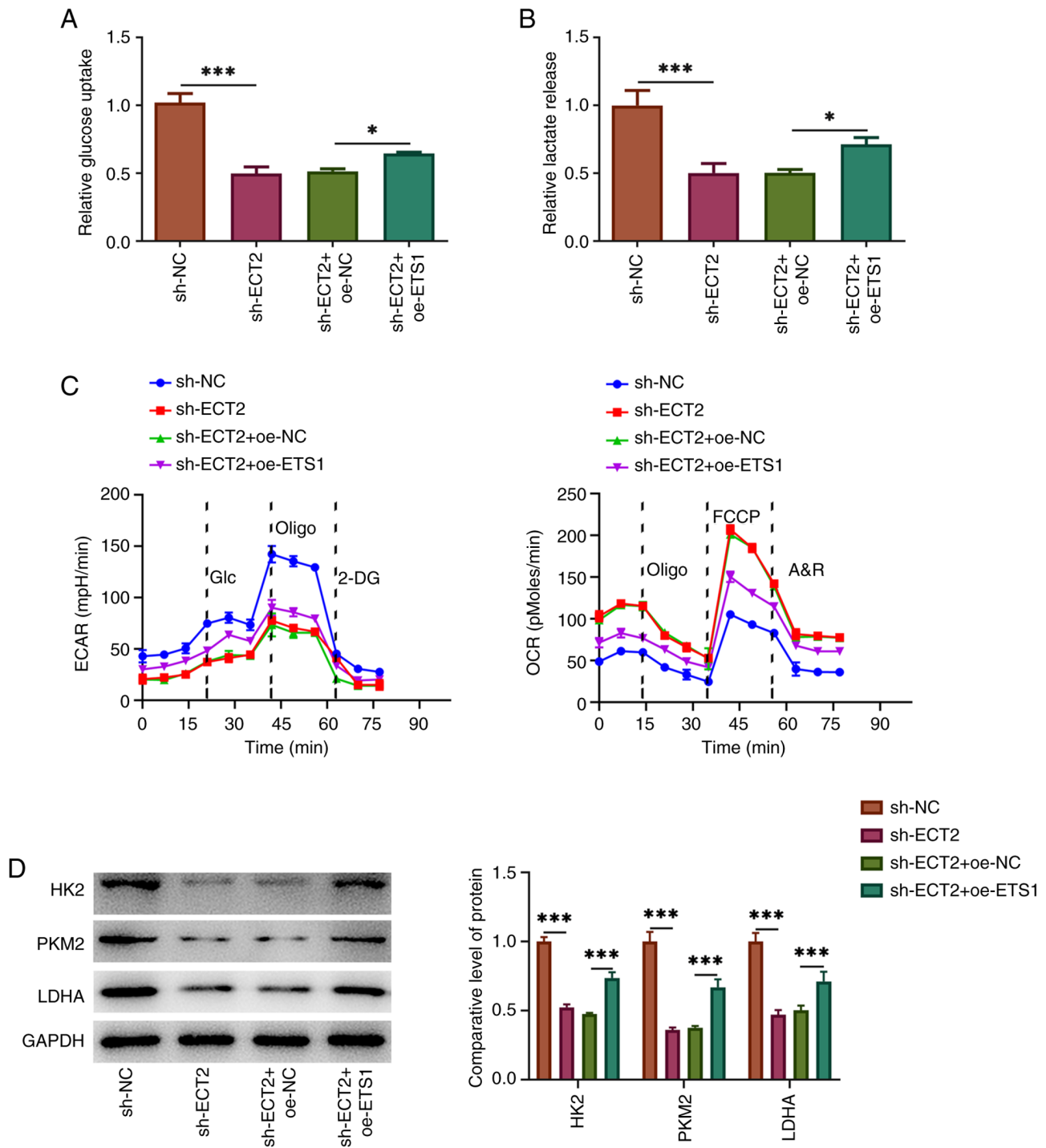


Figure 6. Impact of knockdown of ECT2 expression on aerobic glycolysis in PC-3 cells is weakened by ETS1 overexpression. The cell culture medium was harvested and the (A) lactate release and (B) glucose uptake were examined using commercial kits. (C) The ECAR and OCR of PC-3 cells were assessed using a Seahorse XFe96 Analyzer to evaluate the glycolytic capacity and maximal respiration. (D) Western blotting was performed to examine the expression levels of several critical enzymes in the aerobic glycolysis process. * $P < 0.05$ and *** $P < 0.001$. 2-DG, 2-deoxy-D-glucose; A&R, antimycin A/rotenone; ECAR, extracellular acidification rate; ECT2, epithelial cell transforming sequence 2; FCCP, carbonylcyanide-4-(trifluoromethoxy) phenylhydrazone; Glc, glucose; HK2, hexokinase 2; LDHA, lactate dehydrogenase A; NC, negative control; OCR, oxygen consumption rate; oe, overexpression vector; Oligo, oligomycin; PKM2, pyruvate kinase M2; sh, short hairpin RNA.

OCR, revealing that the inhibitory effect of knockdown of ECT2 expression on aerobic glycolysis was partly weakened by ETS1 overexpression (Fig. 6A-C). Furthermore, ECT2 knockdown-reduced protein expression levels of HK2, PKM2 and LDHA were partly restored by additional ETS1 overexpression (Fig. 6D).

Discussion

Prostate cancer is the most common cancer in men worldwide (1,2). It is of great importance to identify novel biomarkers and develop effective therapeutic targets for the treatment of prostate cancer. The present study demonstrated that ECT2

was highly expressed in prostate cancer. Knockdown of ECT2 expression could reduce aerobic glycolysis of prostate cancer, and thus, inhibit cell proliferation, invasion and migration. Furthermore, the transcription factor ETS1 could directly bind to the ECT2 promoter and positively regulate ECT2. The regulatory role of ECT2 in prostate cancer may be partly mediated by ETS1. Taken together, the data demonstrated that ECT2 may be a promising therapeutic target in human prostate cancer.

Numerous studies have shown that cancer cells reprogram their metabolism to facilitate growth, survival and metastasis (19,20). The alteration of aerobic glycolysis, also known as the 'Warburg effect', is a well-recognized hallmark of cancer cell metabolism (20). Increased glycolysis, which is accompanied by increased glucose intake and fermentation of glucose to lactate, is essential to fulfill the demands of energy requirements and macromolecule synthesis in cancer cells, and it also modulates the tumor stroma to a pro-tumorigenic microenvironment, thereby promoting cancer cell proliferation (21,22). Therefore, restriction of aerobic glycolysis may provide possible therapeutic targets or drugs for cancer therapy (22-24). At present, the role of ECT2 in glucose metabolic reprogramming of cancer has not been fully investigated. The limited findings have revealed that ECT2 could enhance aerobic glycolysis to promote the M2 phenotype polarization of tumor-associated macrophages in hepatocellular carcinoma, thereby promoting the proliferation and migration of hepatocellular carcinoma cells (25). Furthermore, Rac GTPase-activating protein 1 has been regarded as a critical driver to promote breast cancer metastasis, which is dependent on ECT2-mediated mitochondrial quality control and aerobic glycolysis (26). Nevertheless, to the best of our knowledge, the association between ECT2 and prostate cancer remains unclear. The present study demonstrated that ECT2 expression was increased in prostate cancer cells. Knockdown of ECT2 expression exhibited significant inhibitory effects on glucose uptake, lactate production and the expression of key glycolytic enzymes (HK2, PKM2 and LDHA), reducing glycolytic metabolite levels, and thus, inhibiting the proliferation, migration and invasion of prostate cancer cells, and delaying the progression of prostate cancer.

Transcription factors are involved in the formation of transcription initiation complexes, and thus, serve important roles in modulating gene expression (27). ETS1 belongs to the ETS family of transcription factors, characterized by a DNA-binding domain containing a GGAA/T core motif (28). Previous studies have identified that ETS1 functions as a crucial transcription factor in various physiological processes in living organisms, such as cell survival, differentiation and apoptosis; therefore, it is regarded to be involved in multiple physiological and pathological processes, such as reproduction, diabetic nephropathy and malignant cancer types (29-31). The regulatory role of ETS1 in carcinoma has been extensively studied (32-34), including in prostate cancer. The transcriptional activity of ETS1 is enhanced in advanced prostate cancer and ETS1 expression is highest in high-grade prostate cancer. *In vitro* functional experiments have demonstrated that elevated ETS1 expression facilitated an aggressive and castrate-resistant phenotype in prostate cancer cells, indicating the oncogenic role of ETS1 transcriptional activity in prostate cancer (34). Circular RNA_0004296 has

been found to inhibit metastasis of prostate cancer, which was largely associated with inhibition of ETS1 mRNA expression (35). Accordingly, the present study revealed high ETS1 expression in prostate cancer cells. A critical binding relationship was confirmed between the transcription factor ETS1 and the ECT2 promoter, and ETS1 could positively regulate ECT2 expression in prostate cancer cells. The subsequent rescue experiments revealed that the inhibitory effects of knockdown of ECT2 expression on cell proliferation, migration, invasion and aerobic glycolysis were reversed by ETS1 overexpression, suggesting that the effect of ECT2 expression on prostate cancer cells was partly mediated by ETS1.

To the best of our knowledge, the present study was the first to reveal the regulatory role of ECT2 in prostate cancer, as well as its potential mechanism of action. The findings revealed that knockdown of ECT2 expression may reduce aerobic glycolysis of prostate cancer, and thus, reduce cell proliferation and invasion, thereby inhibiting prostate cancer progression (19,36). With regard to its mechanism of action, ECT2 was transcriptionally activated by the transcription factor ETS1. The present study provided a potential biomarker and therapeutic target for patients with prostate cancer.

There were some limitations in the present study. Although the oncogenic role of ETS1 has been confirmed previously (34,35), re-examination of ETS1 expression in prostate cancer cells could further validate the existing evidence, and would be beneficial to confirm the regulation of ETS1/ECT2 in prostate cancer. Animal experiments may be conducted in future work to further verify the current findings, and clinical verification should also be considered.

Acknowledgements

Not applicable.

Funding

The present study was supported by Xiamen Natural Science Foundation (grant no. 3502Z20227422).

Availability of data and materials

The data generated in the present study may be requested from the corresponding author.

Authors' contributions

BZ, KC and JC designed the study. BZ, KC, XL, ZW, YW, LX, JX and JC performed the experiments to collect and analyze the data. BZ and KC drafted the manuscript and JC revised the manuscript. BZ, KC and JC confirm the authenticity of all the raw data. All authors read and approved the final manuscript.

Ethics approval and consent to participate

Not applicable.

Patient consent for publication

Not applicable.

Competing interests

The authors declare that they have no competing interests.

References

1. Adamaki M and Zoumpourlis V: Prostate cancer biomarkers: From diagnosis to prognosis and precision-guided therapeutics. *Pharmacol Ther* 228: 107932, 2021.
2. Uhr A, Glick L and Gomella LG: An overview of biomarkers in the diagnosis and management of prostate cancer. *Can J Urol* 27 (S3): 24-27, 2020.
3. Siegel RL, Miller KD, Wagle NS and Jemal A: Cancer statistics, 2023. *CA Cancer J Clin* 73: 17-48, 2023.
4. Culp MB, Soerjomataram I, Efstathiou JA, Bray F and Jemal A: Recent global patterns in prostate cancer incidence and mortality rates. *Eur Urol* 77: 38-52, 2020.
5. Howard N, Clementino M, Kim D, Wang L, Verma A, Shi X, Zhang Z and DiPaola RS: New developments in mechanisms of prostate cancer progression. *Semin Cancer Biol* 57: 111-116, 2019.
6. Bhoir S and De Benedetti A: Targeting prostate cancer, the 'tousled way'. *Int J Mol Sci* 24: 11100, 2023.
7. Sehrawat A, Gao L, Wang Y, Bankhead A III, McWeeney SK, King CJ, Schwartzman J, Urrutia J, Bisson WH, Coleman DJ, *et al*: LSD1 activates a lethal prostate cancer gene network independently of its demethylase function. *Proc Natl Acad Sci USA* 115: E4179-E4188, 2018.
8. Fields AP and Justilien V: The guanine nucleotide exchange factor (GEF) Ect2 is an oncogene in human cancer. *Adv Enzyme Regul* 50: 190-200, 2010.
9. Saito S, Liu XF, Kamijo K, Raziuddin R, Tatsumoto T, Okamoto I, Chen X, Lee CC, Lorenzi MV, Ohara N and Miki T: Deregulation and mislocalization of the cytokinesis regulator ECT2 activate the Rho signaling pathways leading to malignant transformation. *J Biol Chem* 279: 7169-7179, 2004.
10. Schneid S, Wolff F, Buchner K, Bertram N, Baygun S, Barbosa P, Mangal S and Zanin E: The BRCT domains of ECT2 have distinct functions during cytokinesis. *Cell Rep* 34: 108805, 2021.
11. Cook DR, Kang M, Martin TD, Galanko JA, Loeza GH, Trembath DG, Justilien V, Pickering KA, Vincent DF, Jarosch A, *et al*: Aberrant expression and subcellular localization of ECT2 drives colorectal cancer progression and growth. *Cancer Res* 82: 90-104, 2022.
12. Zhang H, Geng Y, Sun C and Yu J: Upregulation of ECT2 predicts adverse clinical outcomes and increases 5-fluorouracil resistance in gastric cancer patients. *J Oncol* 2021: 2102890, 2021.
13. Sun BY, Wei QQ, Liu CX, Zhang L, Luo G, Li T and Lü MH: ECT2 promotes proliferation and metastasis of esophageal squamous cell carcinoma via the RhoA-ERK signaling pathway. *Eur Rev Med Pharmacol Sci* 24: 7991-8000, 2020.
14. Yi M, Zhang D, Song B, Zhao B, Niu M, Wu Y, Dai Z and Wu K: Increased expression of ECT2 predicts the poor prognosis of breast cancer patients. *Exp Hematol Oncol* 11: 107, 2022.
15. Guo Z, Chen X, Du T, Zhu D, Lai Y, Dong W, Wu W, Lin C, Liu L and Huang H: Elevated levels of epithelial cell transforming sequence 2 predicts poor prognosis for prostate cancer. *Med Oncol* 34: 13, 2017.
16. Chandrashekar DS, Karthikeyan SK, Korla PK, Patel H, Shovon AR, Athar M, Netto GJ, Qin ZS, Kumar S, Manne U, *et al*: UALCAN: An update to the integrated cancer data analysis platform. *Neoplasia* 25: 18-27, 2022.
17. Livak KJ and Schmittgen TD: Analysis of relative gene expression data using real-time quantitative PCR and the 2(-Delta Delta C(T)) Method. *Methods* 25: 402-408, 2001.
18. Zhang Y and Weinberg RA: Epithelial-to-mesenchymal transition in cancer: Complexity and opportunities. *Front Med* 12: 361-373, 2018.
19. Cai K, Chen S, Zhu C, Li L, Yu C, He Z and Sun C: FOXD1 facilitates pancreatic cancer cell proliferation, invasion, and metastasis by regulating GLUT1-mediated aerobic glycolysis. *Cell Death Dis* 13: 765, 2022.
20. Vander Heiden MG, Cantley LC and Thompson CB: Understanding the Warburg effect: The metabolic requirements of cell proliferation. *Science* 324: 1029-1033, 2009.
21. DeBerardinis RJ, Lum JJ, Hatzivassiliou G and Thompson CB: The biology of cancer: Metabolic reprogramming fuels cell growth and proliferation. *Cell Metab* 7: 11-20, 2008.
22. Chelakkot C, Chelakkot VS, Shin Y and Song K: Modulating glycolysis to improve cancer therapy. *Int J Mol Sci* 24: 2606, 2023.
23. Li L, Liang Y, Kang L, Liu Y, Gao S, Chen S, Li Y, You W, Dong Q, Hong T, *et al*: Transcriptional regulation of the warburg effect in cancer by SIX1. *Cancer Cell* 33: 368-385 e7, 2018.
24. Wu Z, Wu J, Zhao Q, Fu S and Jin J: Emerging roles of aerobic glycolysis in breast cancer. *Clin Transl Oncol* 22: 631-646, 2020.
25. Xu D, Wang Y, Wu J, Zhang Z, Chen J, Xie M, Tang R, Chen C, Chen L, Lin S, *et al*: ECT2 overexpression promotes the polarization of tumor-associated macrophages in hepatocellular carcinoma via the ECT2/PLK1/PTEN pathway. *Cell Death Dis* 12: 162, 2021.
26. Ren K, Zhou D, Wang M, Li E, Hou C, Su Y, Zou Q, Zhou P and Liu X: RACGAP1 modulates ECT2-Dependent mitochondrial quality control to drive breast cancer metastasis. *Exp Cell Res* 400: 112493, 2021.
27. Zhi T, Jiang K, Xu X, Yu T, Zhou F, Wang Y, Liu N and Zhang J: ECT2/PSMD14/PTTG1 axis promotes the proliferation of glioma through stabilizing E2F1. *Neuro Oncol* 21: 462-473, 2019.
28. Wang S, Linde MH, Munde M, Carvalho VD, Wilson WD and Poon GM: Mechanistic heterogeneity in site recognition by the structurally homologous DNA-binding domains of the ETS family transcription factors Ets-1 and PU.1. *J Biol Chem* 289: 21605-21616, 2014.
29. Geng XD, Wang WW, Feng Z, Liu R, Cheng XL, Shen WJ, Dong ZY, Cai GY, Chen XM, Hong Q and Wu D: Identification of key genes and pathways in diabetic nephropathy by bioinformatics analysis. *J Diabetes Investig* 10: 972-984, 2019.
30. Chakraborty S and Banerjee S: Multidimensional computational study to understand non-coding RNA interactions in breast cancer metastasis. *Sci Rep* 13: 15771, 2023.
31. Yang F, Liu Y, Wang P, Wang X, Chu M and Wang P: Mutation of the ETS1 3'UTR interacts with miR-216a-3p to regulate granulosa cell apoptosis in sheep. *Theriogenology* 210: 133-142, 2023.
32. Dittmer J: The role of the transcription factor Ets1 in carcinoma. *Semin Cancer Biol* 35: 20-38, 2015.
33. Chen Y, Peng C, Chen J, Chen D, Yang B, He B, Hu W, Zhang Y, Liu H, Dai L, *et al*: WTAP facilitates progression of hepatocellular carcinoma via m6A-HuR-dependent epigenetic silencing of ETS1. *Mol Cancer* 18: 127, 2019.
34. Smith AM, Findlay VJ, Bandurraga SG, Kistner-Griffin E, Spruill LS, Liu A, Golshayan AR and Turner DP: ETS1 transcriptional activity is increased in advanced prostate cancer and promotes the castrate-resistant phenotype. *Carcinogenesis* 33: 572-580, 2012.
35. Mao S, Zhang W, Yang F, Guo Y, Wang H, Wu Y, Wang R, Maskey N, Zheng Z, Li C, *et al*: Hsa_circ_0004296 inhibits metastasis of prostate cancer by interacting with EIF4A3 to prevent nuclear export of ETS1 mRNA. *J Exp Clin Cancer Res* 40: 336, 2021.
36. Xu W, Zeng F, Li S, Li G, Lai X, Wang QJ and Deng F: Crosstalk of protein kinase C ε with Smad2/3 promotes tumor cell proliferation in prostate cancer cells by enhancing aerobic glycolysis. *Cell Mol Life Sci* 75: 4583-4598, 2018.



Copyright © 2024 Zheng et al. This work is licensed under a Creative Commons Attribution-NonCommercial-NoDerivatives 4.0 International (CC BY-NC-ND 4.0) License.